Variational Monte Carlo method for shell-model calculations in odd-mass nuclei and restoration of symmetry

Noritaka Shimizu
Center for Nuclear Study, The University of Tokyo, 7-3-1 Hongo, Bunkyo-ku, Tokyo 113-0033, Japan

Takahiro Mizusaki
Institute of Natural Sciences, Senshu University, 3-8-1 Kanda-Jinbocho, Chiyoda-ku, Tokyo 101-8425, Japan

(Received 3 August 2018; published 15 November 2018)

Background: While a large-scale shell model calculation (LSSM) is a powerful model to describe the nuclear spectroscopic information, it requires a huge amount of computational resources. As an efficient approximation framework to the LSSM, we have introduced the variational Monte Carlo (VMC) method [T. Mizusaki *et al.*, Phys. Rev. C **85**, 021301(R) (2012)]. However, this framework was applicable only to even-mass nuclei.
Purpose: We aim to extend the VMC method for better precision and to make it applicable to odd-mass nuclei.
Methods: We investigate two kinds of extensions for the VMC method with the Pfaffian in the nuclear shell-model calculations. One is the extension to odd-mass nuclei, for which we find a new Pfaffian expression of the VMC matrix elements. The other is the extension of the variation after angular-momentum projection.
Results: We successfully implement the full angular-momentum projected trial state into the VMC method, which can provide us with precise yrast energies. We also find a unique characteristic, namely that this angular-momentum projection in the VMC can be even "approximately" performed.
Conclusions: A unified VMC framework with the variation after projection is given both for even and odd-mass nuclei. The approximate angular-momentum projection is useful not only for efficient computation but also for precise estimation of the yrast energies through the energy-variance extrapolation.

DOI: 10.1103/PhysRevC.98.054309

I. INTRODUCTION

Variational Monte Carlo is one of the quantum Monte Carlo methods to solve quantum many-body problems numerically. While it is a variational method and the precision of the approximation depends on the quality of the trial wave function and the Hamiltonian, it is applicable to any Hamiltonian without the notorious sign problem. Therefore, it has been intensively developed in various fields, such as condensed matter physics [1–4] and nuclear physics [5,6]. Especially, the advent of the stochastic reconfiguration (SR) method [7] enables us to use a large number of variational parameters efficiently. Moreover, as a trial state, a particle-number-projected Hartree-Fock-Bogoliubov (HFB) wave function can be used owing to the Pfaffian, which is known to provide us with a compact and computationally effective wave function [8]. This recent progress broadens the applicability to the configuration-space methods, such as the Hubbard model.

In nuclear physics, the large-scale shell-model (LSSM) calculation is one of the configuration-space methods, and is a powerful model to describe the nuclear spectroscopic information precisely. However, the number of many-body configurations which appear in the LSSM tends to be huge, and the dimension of the Hamiltonian matrix to be diagonalized often surpasses the capability of state-of-the-art supercomputers [9]. In order to avoid this problem and to describe the shell-model wave function in a sophisticated form, the pair-correlated wave function, or the HFB-type wave function, was suggested in the VAMPIR method [10]. However, the HFB wave function is awkward for treating odd-mass systems [11]. We have proposed a new formulation of the variational Monte Carlo (VMC) method for shell-model calculations for even-mass nuclei [6] and demonstrated its feasibility for LSSM calculations.

In the present paper, we address two kinds of extensions of the previously presented VMC method. One extension is to handle odd-mass nuclei in the framework of VMC with a new Pfaffian expression. We present a common VMC framework both for even and odd-mass nuclei. The other extension is the implementation of the variation after angular-momentum projection. Since the atomic nucleus is an isolated system, the restoration of symmetry is crucial for the nuclear structure calculations [12]. We successfully implement the trial state with full angular-momentum projection into the VMC method. Unlike other applications of angular-momentum projection, we find a unique characteristic that full angular-momentum projection in the VMC can be performed "approximately." This characteristic is useful not only for efficient computation but also for precise estimation of the yrast energies through the energy-variance extrapolation. In condensed matter physics, the projection method was introduced in, e.g., Refs. [13–15], and it was also introduced into the VMC in Ref. [1]. The projection method is well known, but this implementation of the VMC is more flexible than the preceding works. It may be useful to other fields of physics.

This paper is organized as follows: Section II is devoted to explaining the theoretical framework of the VMC method and its extension to odd-mass nuclei. The numerical results and "approximate" projection are discussed in Sec. III. The summary is given in Sec. IV.

II. FORMULATION OF THE VMC

In this section, we briefly describe the formulation of the VMC. We introduce a trial wave function in Sec. II A and describe how to stochastically evaluate the energy expectation value of the wave function in the framework of the Monte Carlo in Sec. II B. The restoration of rotational symmetry by the projection method in the VMC is summarized in Sec. II C. The variational parameters are determined so that the energy is minimized utilizing the SR method, the details of which are given in Appendix C.

A. Trial wave function

As a trial wave function for nuclei with N valence particles for the present VMC, we take $|\psi\rangle$ as

$$|\psi\rangle = GP|\phi\rangle, \tag{1}$$

where the $|\phi\rangle$ is a pair-correlated wave function and P is a projection operator, both of which are discussed later. The operator G is the Gutzwiller-like factor,

$$G = \exp\left(\sum_{i\leqslant j}\alpha_{ij}n_i n_j\right), \tag{2}$$

where n_i is the number operator of the single-particle orbit i and α's are variational parameters.

For even-mass nuclei, the $|\phi\rangle$ is defined as

$$|\phi\rangle = \left(\sum_{kk'} f_{kk'}c_k^\dagger c_{k'}^\dagger\right)^{N/2}|-\rangle, \tag{3}$$

where f is a skew-symmetric matrix, $f_{kk'} = -f_{k'k}$, the matrix elements of which are variational parameters. The $|-\rangle$ is an inert core and the $c_k^\dagger$'s are proton or neutron creation operators of the single-particle state k. It corresponds to the number projected Hartree-Fock-Bogoliubov wave function [16], which is advantageous for the description of pairing correlations. Note that this wave function contains the proton-neutron pairing correlations in addition to the proton-proton and neutron-neutron pairing correlations, while the usual HFB method does not include proton-neutron pairing correlations. It plays a crucial role in understanding the nuclear structure of $N = Z$ nuclei [17,18].

For odd-mass nuclei, we extend the trial wave function $|\phi\rangle$, which is defined as

$$|\phi\rangle = \left(\sum_l h_l c_l^\dagger\right)\left(\sum_{kk'} f_{kk'}c_k^\dagger c_{k'}^\dagger\right)^{(N-1)/2}|-\rangle, \tag{4}$$

where the h_l are additional variational parameters. This form is the simplest for odd-mass nuclei. Hereafter we discuss the VMC formalism for the odd-mass cases. The formulation of the even-mass case can be seen in Ref. [6] and is also obtained easily by omitting the terms containing the h_l parameters in the following formulations; that is, we can give a unified description with this trial wave function for even- and odd-mass nuclei.

The projection operator P serves to restore the rotational symmetry, parity symmetry, and z component of isospin, as

$$P = P^{T_z}P^\pi P^I_M, \tag{5}$$

where P^{T_z}, P^π, and P^I_M are projectors of the z component of the isospin, the parity π, and the total angular momentum (I, M), respectively. The angular-momentum operator is decomposed into the $\langle J_z\rangle = M$ projection and the rest as

$$P^I_M = P_M\tilde{P}^I_M, \tag{6}$$

where

$$\tilde{P}^I_M \equiv \frac{2I+1}{4\pi}\sum_{K=-I}^{I} g_K\int d\gamma\, d\beta \sin\beta d^I_{MK}(\beta)e^{-iK\gamma}e^{iJ_y\beta}e^{iJ_z\gamma}. \tag{7}$$

The $d^I_{MK}(\beta)$ is Wigner's d function and g_K denotes the $2I+1$ variational parameters.

B. Markov chain Monte Carlo method

We describe how to estimate the energy expectation value of the trial wave function. First of all, the projection operator of the z component of isospin, parity, and z component of angular momentum is expressed as a linear combination of the complete set in the m-scheme basis states as

$$P^{T_z}P^\pi P_M = \sum_{m\in\{M^\pi\}}|m\rangle\langle m|, \tag{8}$$

where the m-scheme basis state $|m\rangle$ is defined as

$$|m\rangle = c^\dagger_{m_1}c^\dagger_{m_2}\cdots c^\dagger_{m_N}|-\rangle, \tag{9}$$

which is parametrized by a set of occupied single-particle states, $m = \{m_1, m_2, \ldots, m_N\}$. The $\sum_{m\in M^\pi}$ denotes the summation of any $|m\rangle$ in the subspace with $J_z = M$ and π parity. It is convenient to take $M = I$, especially for the yrast states.

The energy expectation value is obtained as

$$\begin{aligned}\langle H\rangle &= \frac{1}{\sum_{m\in M^\pi}|\langle m|\psi\rangle|^2}\sum_{m\in M^\pi}|\langle m|\psi\rangle|^2\frac{\langle m|H|\psi\rangle}{\langle m|\psi\rangle}\\ &= \sum_{m\in M^\pi}p(m)E_l(m),\end{aligned} \tag{10}$$

where $p(m)$ is defined as $p(m) = |\langle m|\psi\rangle|^2/\sum_m|\langle m|\psi\rangle|^2$. $E_l(m)$ is called the local energy and is defined as

$$E_l(m) = \frac{\langle m|H|\psi\rangle}{\langle m|\psi\rangle} = \frac{1}{\langle m|\psi\rangle}\sum_{m'\in M^\pi}\langle m|H|m'\rangle\langle m'|\psi\rangle, \tag{11}$$

where the matrix $H_{mm'} = \langle m|H|m'\rangle$ is sparse and the summation concerning m' can be computed efficiently since the shell-model Hamiltonian H is a two-body interaction and has good parity and rotational symmetries. The matrix element $\langle m|H|m'\rangle$ itself is also computed efficiently: in the practical code, $|m\rangle$ is expressed as the array of $(m_1, m_2, \ldots, m_N)$ and

we operate each of the two-body terms of the Hamiltonian operator in a way similar to the conventional Lanczos shell-model codes [9,19].

The weighted summation $\sum_m p(m)$ in Eq. (10) is estimated stochastically using the Markov chain Monte Carlo (MCMC) method in which $|m\rangle$ walks randomly in the $\{M^\pi\}$ subspace obeying the probability $p(m)$. Such a random walker of the m-scheme basis state was adopted also in Refs. [6,20,21]. The energy gradient and the overlap matrix are also estimated stochastically by the SR method.

The overlap between the m-scheme basis state and $|\psi\rangle$ is shown by

$$\langle m|\psi\rangle = G(m)\langle m|P|\phi\rangle \tag{12}$$

with $G|m\rangle = G(m)|m\rangle$. Note that G is a diagonal operator for the m-scheme basis representation and is commutable with the projection operator P. This factor usually accelerates the convergence of the SR iterations. While this operator can include many-body correlation beyond the mean-field and pairing correlations, its contribution to the energy gain is limited in the case of shell-model calculations. The projected overlap, $\langle m|P|\phi\rangle$, is discussed in the following subsection.

C. Angular-momentum projection

The projected overlap $\langle m|P|\phi\rangle$ is evaluated as

$$\begin{aligned}\langle m|P|\phi\rangle &= \langle m|\tilde{P}^I_M|\phi\rangle \\ &= \frac{2I+1}{4\pi}\int d(\cos\beta)d\gamma d^I_{MK}(\beta)e^{-iK\gamma}\langle m|R(\beta,\gamma)|\phi\rangle \\ &\simeq \frac{2I+1}{4\pi}\sum_K g_K \sum_a^{N_z} w_a^{(z)} e^{-iK\gamma_a}\sum_b^{N_y} w_b^{(y)} d^I_{MK}(\beta_b) \\ &\quad\times\langle m|R(\beta_b,\gamma_a)|\phi\rangle,\end{aligned} \tag{13}$$

where the integrals over $\cos\beta$ and γ are numerically approximated by weighted sums. The points (γ_b, β_a) and its weight factors $(w_a^{(z)}, w_b^{(y)})$ for the integrals are determined by the trapezoidal rule for γ and the Gauss-Legendre quadrature for $\cos(\beta)$ [22] for efficient computation. The number of the points for integrals, N_z and N_y, are usually determined to be large enough to evaluate the correct expectation value of J^2. The numbers are taken typically as $(N_z, N_y) = (32, 16)$. The rotation of the correlated-pair wave function $|\phi\rangle$ is evaluated as

$$\begin{aligned}R(\beta,\gamma)|\phi\rangle &= e^{iJ_y\beta_b}e^{iJ_z\gamma_a}|\phi\rangle \\ &= \left(\sum_l h'_l c^\dagger_l\right)\left(\sum_{kk'} f'_{kk'}c^\dagger_k c^\dagger_{k'}\right)^{(N-1)/2}|-\rangle\end{aligned} \tag{14}$$

with $h' = Rh$, $f' = RfR^T$. The rotation matrix R is defined as $R = e^{J_y\beta_b}e^{J_z\gamma_a}$. Thus the rotated wave function is kept in the same form thanks to the Baker-Campbell-Hausdorff theorem [23].

In this paper, we find that the overlap between this form of the wave function $|\phi\rangle$ and the m-scheme basis state can be written using the single Pfaffian. This is shown in Appendix A.

The variational parameters α, h, f, and g are determined so that the energy is minimized utilizing the SR method. In this paper, we show that the angular-momentum projected energy can be minimized in the VAP framework of the VMC, while the unprojected energy is also minimized to determine the wave function, and the projected energy can be evaluated in the variation-before-projection (VBP) framework [6]. In the VMC approach, "unprojected" means without full-angular-momentum projector $\tilde{P}^I_M$, but with the J_z, parity, and T_z projections.

III. NUMERICAL RESULTS

We discuss the VMC results with variation after angular-momentum projection (J-VAP) in the even-mass case in Sec. III A and in the odd-mass case in Sec, III B. The J-VAP calculation can give better yrast energies than those of our previous paper [6], while it requires a more substantial computational cost. In Sec. III C, the "approximation" scheme of angular-momentum projection is introduced to reduce the computational cost. We show that this approximation scheme can give a sequence of wave functions, which can be useful for the extrapolation using the energy variance. With the energy variance extrapolation, the exact yrast energies can be estimated beyond the limitation of the trial wave function.

A. Variation after projection for even-mass nuclei

In this subsection, we demonstrate the VAP calculation with the variation after angular-momentum projection of ^{48}Cr in the pf shell. The GXPF1A interaction is adopted as an effective interaction [24]. The m-scheme dimension of the $M = 0$ subspace is 1 963 461. While it is tractable for the conventional shell-model calculations, the shell-model calculation of ^{48}Cr has been used for benchmark tests of various shell-model-based methods [9]. For the test of the VMC calculation, we use a realistic residual interaction, not a schematic interaction, in order to properly judge the feasibility of the method.

Figure 1 shows the convergence of the VMC energy with full angular-momentum projection, which is called J-VAP VMC energy later, as a function of the number of the iterations of the SR method. The MCMC procedure generates eight random walkers with 8000 steps with the Gibbs sampler, the details of which are shown in Ref. [6]. This step needs twofold integration over Euler's angle as in Eq. (13), which needs heavy numerical computation. At the present stage, the computation time of the VMC is not very competitive with the exact shell-model calculation using the Lanczos method. For example, the VMC calculation to obtain the 0^+ state of ^{48}Cr costs 176 seconds on a PC server with 56 CPU cores, while the Lanczos calculation requires 12 seconds using the shell-model code KSHELL [25]. However, the Lanczos calculation has a difficulty due to the explosive increase of the m-scheme dimension in mid-shell nuclei, while the computation amount of VMC is expected to be much more modestly increased. In addition, we will show how to reduce the amount of the VMC computation in Sec. III C.

The convergence of the J-VAP VMC energies is almost achieved with up to 50–60 steps. Since the Monte Carlo

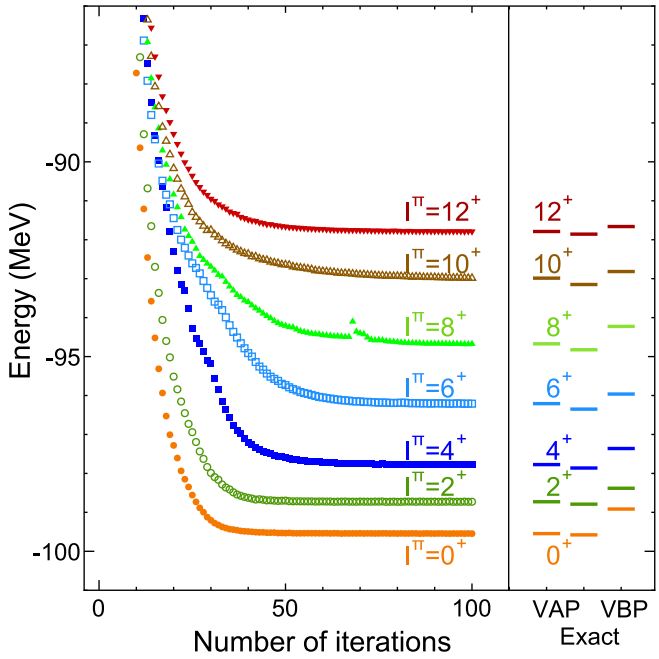

FIG. 1. Convergence of energies of $I^\pi = 0^+$ (filled orange circles), 2^+ (open green circles), 4^+ (filled blue squares), 6^+ (open light-blue squares), 8^+ (filled green triangles), 10^+ (open brown triangles), and 12^+ (filled red inverted triangles) states of ^{48}Cr obtained by J-VAP VMC as functions of the number ofe SR iterations. The right column shows the VAP results, exact shell-model energies, and the VBP results of the $I^\pi = 0^+$, 2^+, 4^+, 6^+, 8^+, 10^+, and 12^+ states in order from the bottom.

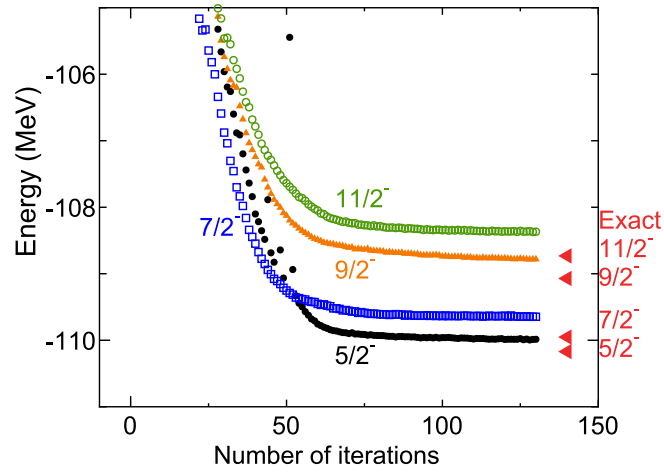

FIG. 2. Convergence of the J-VAP VMC energies of ^{49}Cr with GXPF1A interaction. The figure shows the energy expectation values of $5/2^-$ (filled black circles), $7/2^-$ (open blue squares), $9/2^-$ (filled orange triangles), and $11/2^-$ (open green circles) states, respectively, as functions of the number of iterations. The exact shell-model energies are shown as the rightmost red triangles.

error of the energy is typically 2 keV and small enough, the error bars are omitted for simplicity in the figure. The J-VAP VMC energy converges well and is close enough to the exact shell-model energies within 160 keV from 0^+ to 12^+ states. For comparison, we show the VBP energy as the rightmost levels in the figure. The VMC with VAP improves the energy over VBP as expected. Especially the VBP result underestimates the 2^+ excitation energy, while the VAP result sufficiently reproduces the exact values including the backbending phenomenon [12]; e.g. $\mathrm{Ex}(12^+) - \mathrm{Ex}(10^+)$ is smaller than $\mathrm{Ex}(10^+) - \mathrm{Ex}(8^+)$. Note that the isoscalar pairing plays an important role in the backbending of ^{48}Cr [26,27] and it is shown that the VMC calculations are suitable for including the isoscalar-pairing correlations. The small energy differences between the exact energies and J-VAP VMC ones will be discussed in Sec. III D.

B. Variation after projection for odd-mass nuclei

In this subsection, we consider the odd-mass nuclei for a test of the new trial wave function. We calculate the yrast energies of ^{49}Cr within the pf-shell model space and the GXPF1A interaction [24]. The m-scheme dimension of the $M = \frac{1}{2}$ subspace reaches 6 004 205. In this VMC calculation, we apply the full angular-momentum projection to the trial state. In the MCMC process, we adopt the Gibbs sampler with 640 random walkers, each of which contains 500 sample steps after 100 burn-in steps. In order to suppress the biases induced by the initial state of the Markov Chain, we take the last sample of the previous SR iteration as an initial sample of the MCMC process.

Figure 2 shows the convergence of the J-VAP VMC energy of ^{49}Cr as an example of odd-mass nuclei. The energies of the yrast states $5/2^-$, $7/2^-$, $9/2^-$, and $11/2^-$ are shown in the figure. The difference between the converged energy and the exact one is similar to the one of the even case, which means that our trial wave function (4) is considerably more proper. However, the number of iterations of the odd case is larger than the one of the even case.

C. Approximate angular-momentum projection

Since the correlated-pair wave function $|\psi\rangle$ does not have good rotational and parity symmetries, the solution spontaneously breaks these symmetries, and it is crucial to restore them by the projection method. In general, J-VAP has a large effect of minimizing the energy in the context of the configuration-interaction approach. Various variational calculation after the angular-momentum projection have therefore been proposed, such as the Monte Carlo shell model [28], the VAMPIR approach [10], and the hybrid multideterminant method [29].

In these J-VAP calculations, since the energy and the energy gradient are computed under the mathematical conditions $[H, P^I_{MK}] = 0$ and $P^I_{ML} P^I_{L'K} = \delta_{LL'} P^I_{MK}$, the high-precision numerical evaluation of the projection is essential. The insufficient number of points for the integral of the Euler angles causes numerical instability, and the angular-momentum projection fails in solving the Hill-Wheeler equation. The angular-momentum projection is, therefore, a central bottleneck of the computation of various variational approaches to the nuclear quantum many-body solver [30].

On the other hand, in the VMC formalism, since the conditions $[H, P^I_{MK}] = 0$ and $P^I_{ML} P^I_{L'K} = \delta_{LL'} P^I_{MK}$ are

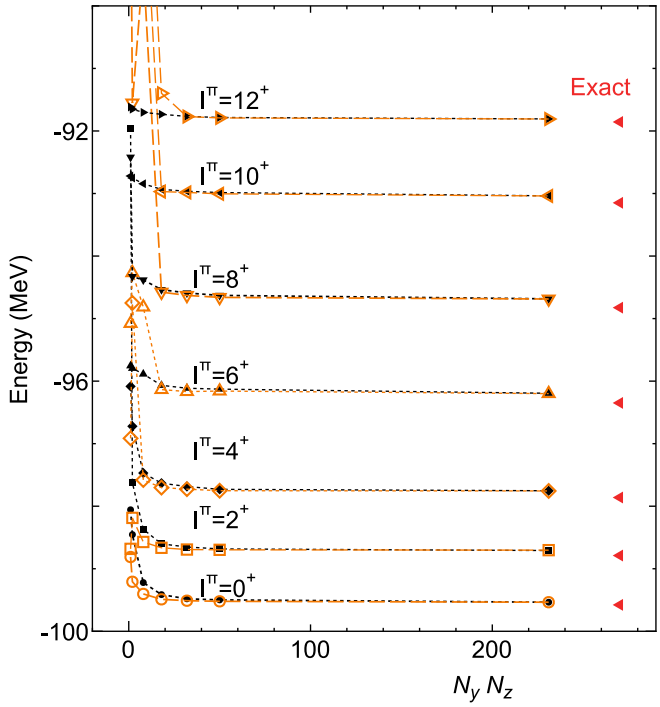

FIG. 3. VMC results with the variation after approximate angular-momentum projection against the total number of the mesh points for the integral, N_zN_y. The filled black symbols connected with the dotted lines denote the converged results of the $I^\pi = 0^+$, 2^+, 4^+, 6^+, 8^+, 10^+, and 12^+ states of ^{48}Cr with the GXPF1A interaction [24]. The open orange symbols connected with the dashed lines denote the fully projected energy of the resultant wave function. See text for further details.

not adopted, high precision calculations for the angular-momentum projection $\tilde{P}^I_M$ are not necessarily needed, which means that the number of mesh points for numerical integration could be reduced. In fact, even when we use a small number of points for the integrals and the operator $\tilde{P}^I_M$ is mathematically no longer valid as a projection operator, $\tilde{P}^I_M|\phi\rangle$ works as a trial wave function with "approximated" angular momentum, because this wave function is simply a superposition of the rotated wave functions of $|\phi\rangle$ with appropriate weight coefficients:

$$\tilde{P}^I_M|\phi\rangle \simeq \sum_{a=1}^{N_z}\sum_{b=1}^{N_y} w_a^{(z)} w_b^{(y)} R(\beta_b, \gamma_a)|\phi\rangle. \tag{15}$$

Therefore, as an approximation to the projection operator, we introduce the $\tilde{P}^I_M$ with a set of the small numbers of N_z and N_y and call it $\tilde{P}'^I_M$ hereafter. Note that $\tilde{P}'^I_M$ is still commutable with the operator G for any (N_z, N_y).

Figure 3 shows the converged VMC energies of the 0^+, 2^+, and 4^+ energies in ^{48}Cr with the GXPF1A interaction [24] as functions of the number of points for the integral of the projection operator $\tilde{P}'^I_M$. The VMC calculation was performed with variation after the $\tilde{P}'^I_M$ projection. The number of the points is taken as $(N_z, N_y) = (1, 1)$, (2,1), (4,2), (6,3), (8,4), (10,5), and (21,11). The converged energies of the variation after the approximated projection are shown as the black symbols in Fig. 3. The case of $(N_z, N_y) = (1, 1)$ corresponds to the variation without the angular-momentum projection. In the figure, the rightmost red triangles denote the exact shell-model energies. The VMC results well reproduce the exact ones, even with the small number of N_zN_y. In order to improve the precision of the angular-momentum projection so that the expectation value of J^2 equals $I(I+1)$ exactly to six decimal digits, the necessary number of points is higher than the minimal one given by $(N_z, N_y) = (28, 14)$, (28,14), (31,16), and (35,18) for $I^\pi = 0^+$, 2^+, 4^+, and 6^+ states, respectively.

Astonishingly, the approximated projection works well even for $(N_z, N_y) = (6, 3)$. The total number of points, N_zN_y, is almost proportional to the amount of computations of the projected matrix elements, which is the most time-consuming part of the VMC calculations. Therefore, the computation amount would be dramatically reduced in comparison with the full projection. The required number of points is rather constant as a function of the angular momentum I, while in the case of the full angular-momentum projection the necessary number of points increases as I does. In the VMC calculation, the wave function is analytically restricted to the $\langle J_z\rangle = I$ subspace by the random walkers of m-scheme basis states in Eq. (10). This removes the contamination of the unwanted lower-I states independently of the number of the points and makes the variational calculation stable. The difference of the energies of the J-VAP calculation and unprojected calculation becomes small in the high-I state. However, we should mention that the numerical calculation is stable as far as no higher spin state exists in the region lower in energy than the target state.

Moreover, we apply the $\tilde{P}^I$ projection, in which N_zN_y is large enough to obtain the correct expectation value of J^2 of the resultant wave functions. The orange symbols in Fig. 3 denote the "full" angular-momentum projected energies. They are considered to be the variation after the approximated projection and before the full projection. These energies are quite close to those of the variation after full projection. In practice the energies obtained by the $(N_z, N_y) = (6, 3)$ variation agree with those of J-VAP VMC within 70-keV difference. In some VMC results of the high-I state with small (N_z, N_y), the energies after full projection are worse than those before projection, possibly because g_K in Eq. (7) is optimized by the variation before full projection and thus is not optimized for the full projection.

D. Energy-variance extrapolation

As the VMC is a variational method, it must not necessarily give us exact energies. The obtained energy is an upper limit. To know the exact energy, one useful method is energy-variance extrapolation [7,31–34], which uses a series of the well-approximated wave functions $|\psi_1\rangle$, $|\psi_2\rangle$, … with monotonically decreasing energies $\langle\psi_1|H|\psi_1\rangle > \langle\psi_2|H|\psi_2\rangle > \cdots$. By evaluating the energy variance as $\langle\Delta H^2\rangle = \langle H^2\rangle - \langle H\rangle^2$ for each wave function, we can show a linear or quadratic relation between the energy variances and the energies and show that the energy approaches the exact energy along the sequence. By fitting a second-order polynomial for data points of energy variance and energy, the exact energy

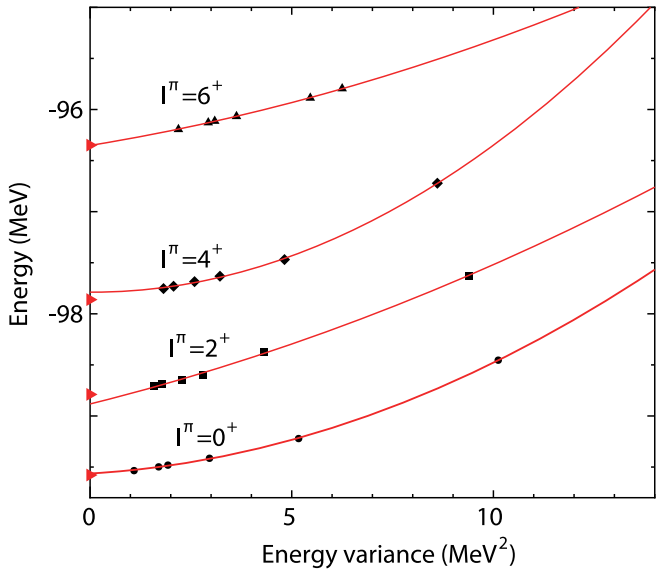

FIG. 4. Energy variance extrapolation by the variation after the approximate angular-momentum projection. The 0^+, 2^+, 4^+, and 6^+ shell-model energies of ^{48}Cr are obtained with the GXPF1A interaction [24]. The energy expectation values against the energy variance are plotted as the black symbols with the approximate projection. The numbers of the points for the projection are taken as $(N_z, N_y) = (2, 1), (4,2), (6,3), (8,4), (10,5)$, and $(21,11)$. The red lines are chi-square-fitted to the symbols. The red squares on the y axis are the exact shell-model energies.

can be expected by extrapolating the energy to the limit of $\langle \Delta H^2 \rangle = 0$.

In the preceding application of the energy-variance extrapolation to the nuclear shell model, we used a truncation scheme concerning particle-hole excitations to prepare the sequence of well-approximated wave functions [34]. In the present J-VAP VMC scheme, the approximate projection method also provides us with a sequence of approximated wave functions by changing the number of points for the integrals. This new method can be applied independently of the underlying shell structure. Figure 4 shows the energy of the VMC with the approximated projection as functions of the expectation value of the energy variance, $\langle \Delta H^2 \rangle = \langle H^2 \rangle - \langle H \rangle^2$. As the number of mesh points increases, the energy expectation values decrease as a function of energy variances and the exact energy is estimated as the intersection of the y axis beyond the limitation of the VMC. These extrapolated energies are close to the exact energies shown as the red symbols on the y axis.

IV. SUMMARY

We presented the VMC method with the Pfaffian to solve the nuclear shell model in Ref. [6], where we handle only even-mass nuclei and variation before angular-momentum projection. In the present paper, we extended the previous VMC method for odd-mass nuclei, by deriving a new Pfaffian expression for the VMC matrix element. We demonstrated that the VMC is successfully applied to odd-mass nuclei. We also extended the VMC to variation after angular-momentum projection, which enhances the quality of the VMC energy.

In addition to these extensions, we also found that the "approximated" angular-momentum projection can work in the VMC framework. So far, no feasible approximation scheme for full angular momentum projection has been presented, and its numerical calculations have been believed to be achievable in quite a strict manner. However, we proposed a novel approximation scheme of angular momentum projection, which reduces the computation drastically and brings about an efficient way to calculate angular momentum projection.

Furthermore, we found that this "approximated" angular-momentum projection also gives a series of well-approximated wave functions, which is useful to the energy variance extrapolation. By this development, we could estimate the exact energies of the shell model beyond the limitation of the VMC method.

The form of the trial wave function can be straightforwardly extended to that of a one-broken-pair state, which is used in the Tamm-Dancoff approximation and shown in Appendix B 3. Its numerical application remains as a future subject.

ACKNOWLEDGMENTS

The authors sincerely acknowledge Professor P. Schuck for carefully reading the manuscript. This work was partly supported by KAKENHI grants (25870168, 17K05433) from JSPS and as a priority issue (Elucidation of the fundamental laws and evolution of the universe, hp170230 and hp180179) to be tackled by using Post K Computer from MEXT and JICFuS. This work was also partly supported by the research grant of the Senshu Research Abroad Program (2018) for one of the authors (T.M.).

APPENDIX A: PFAFFIAN AND ITS RELEVANT FORMULAS

The Pfaffian plays the main role in evaluating the matrix elements which appear in the present VMC formalism. Some useful formulas relevant to the Pfaffian are given in this Appendix. The Pfaffian of a $2n \times 2n$ skew-symmetric matrix A is defined as

$$\mathrm{Pf}(A) \equiv \frac{1}{2^n n!} \sum_{\sigma \in S_{2n}} \mathrm{sgn}(\sigma) \prod_{i=1}^{n} A_{\sigma(2i-1)\sigma(2i)}$$
$$= \frac{1}{n!} \sum_{\sigma \in S_{2n} | \sigma(2i-1) < \sigma(2i)} \mathrm{sgn}(\sigma) \prod_{i=1}^{n} A_{\sigma(2i-1)\sigma(2i)}, \quad \text{(A1)}$$

where σ is a permutation of $\{1, 2, 3, \ldots, 2n\}$, $\mathrm{sgn}(\sigma)$ is its sign, and S_{2n} is a group of the permutations.

For preparation, the recursive relation of Pfaffian is given as

$$\mathrm{Pf}(A) = \sum_{j=1}^{2n} (-1)^{i+j+1+\theta(i-j)} A_{ij} \mathrm{Pf}(A_{\overline{ij}}), \quad \text{(A2)}$$

where $A_{\overline{ij}}$ denotes the matrix A with the ith and jth columns and rows removed. $\theta(i-j)$ is the Heaviside step function. Its

special case with $i = 1$ is written as

$$\mathrm{Pf}(A) = \sum_{j=1}^{2n} (-1)^j A_{1j} \mathrm{Pf}(A_{\overline{1j}}). \tag{A3}$$

The differentiation of the Pfaffian is given by

$$\frac{\partial}{\partial A_{ij}} \mathrm{Pf}(A) = -\mathrm{Pf}(A)(A^{-1})_{ij}. \tag{A4}$$

APPENDIX B: OVERLAP WITH THE TRIAL WAVE FUNCTION AND *m*-SCHEME BASIS STATE

In the present VMC formalism, the overlap between the trial wave function and the m-scheme basis state must be computed efficiently. The trial wave function is a product of the Gutzwiller-like operator G and the pair-correlated wave function. Since the operator G is diagonal in the m-scheme basis, the overlap is factorized into the matrix element of G and the pair-correlated part such as

$$\langle m|\psi\rangle = G(m)\langle m|\phi\rangle \tag{B1}$$

with

$$G(m) = \exp\left(\sum_{i\leqslant j} \alpha_{ij} n_i n_j\right), \tag{B2}$$

where n_i is the number operator of the single-particle orbit i and α's are variational parameters. The differential with respect to the variational parameter α_{ij} is obtained simply as

$$\frac{1}{\langle m|\psi\rangle}\frac{\partial}{\partial \alpha_{ij}}\langle m|\psi\rangle = n_i n_j. \tag{B3}$$

The overlap between the pair-correlated wave functions [e.g., Eqs. (3) and (4)] and m-scheme basis state in Eq. (9) are obtained by using the Pfaffian efficiently. Hereafter we describe the overlap and its derivative concerning the pair-correlated wave functions.

1. Even-mass nuclei

It is useful to obtain the overlap between the m-scheme basis state for the $2n$-valence-particles nuclei in Eq. (3) and the pair-correlated state $|\phi\rangle$. Using Eq. (A1), it is obtained as

$$\langle m|\phi\rangle = \langle m|\left(\sum f_{ij} c_i^\dagger c_j^\dagger\right)^n|-\rangle = n!\,\mathrm{Pf}(F), \tag{B4}$$

where $F_{rs} = f_{m_r m_s} - f_{m_s m_r}$.

Utilizing Eq. (A4), its differential is obtained as

$$\frac{1}{\langle m|\psi\rangle}\frac{\partial}{\partial F_{rs}}\langle m|\psi\rangle = -(F^{-1})_{rs}. \tag{B5}$$

2. Odd-mass nuclei

The correlated wave function for the odd-mass case is defined in Eq. (4). The number of particles is $N = 2n - 1$. As a novelty, we show the overlap between this odd wave function and the m-scheme basis state. Using Eq. (A3), the overlap is obtained as

$$\begin{aligned}\langle m|\phi\rangle &= \langle m|\left(\sum_l h_l c_l^\dagger\right)\left(\sum_{kk'} f_{kk'} c_k^\dagger c_{k'}^\dagger\right)^{n-1}|-\rangle \\ &= n!\,\mathrm{Pf}(F),\end{aligned} \tag{B6}$$

where F is a $n \times n$ skew-symmetric matrix and consists of the first row being h_{m_p} and the others being $\tilde{f}_{ij} = f_{m_i,m_j} - f_{m_j,m_i}$:

$$F = \begin{pmatrix} 0 & h_{m_1} & h_{m_2} & h_{m_3} & \cdots & h_{m_N} \\ -h_{m_1} & 0 & \tilde{f}_{1,2} & \tilde{f}_{1,3} & \cdots & \tilde{f}_{1,N} \\ -h_{m_2} & \tilde{f}_{2,1} & 0 & \tilde{f}_{2,3} & \cdots & \tilde{f}_{2,N} \\ \cdots & & & & \cdots & \\ \cdots & & & & \cdots & \\ -h_{m_N} & \tilde{f}_{N,1} & \tilde{f}_{N,2} & \tilde{f}_{N,3} & \cdots & 0 \end{pmatrix}. \tag{B7}$$

Its differentiation is also obtained in a manner similar to the even-mass case:

$$\begin{aligned}\frac{1}{\langle m|\psi\rangle}\frac{\partial\langle m|\psi\rangle}{\partial h_{m_k}} &= -(F^{-1})_{1,k+1} \\ \frac{1}{\langle m|\psi\rangle}\frac{\partial\langle m|\psi\rangle}{\partial \tilde{f}_{m_k,m_l}} &= -(F^{-1})_{k+1,l+1}.\end{aligned} \tag{B8}$$

3. Tamm-Dancoff wave function

The wave function used in the Tamm-Dancoff approximation, which is called a one-broken-pair state, is a good approximation to the excited state of the pair-condensed wave function in even-mass nuclei having $2n$ valence particles. It can also be used in the VMC formalism, and is defined as

$$|\phi\rangle = \left(\sum_{ll'} h_{ll'} c_l^\dagger c_{l'}^\dagger\right)\left(\sum_{kk'} f_{kk'} c_k^\dagger c_{k'}^\dagger\right)^{n-1}|-\rangle. \tag{B9}$$

Its overlap is obtained using Eq.(A3) as

$$\begin{aligned}\langle m|\phi\rangle &= \sum_{p,q=1}^{2n} (-1)^{p+q-1} h_{m_p m_q} (n-1)!\,\mathrm{Pf}(F^{\overline{m_p m_q}}) \\ &= \sum_{p=1}^{2n} (-1)^p (n-1)!\,\mathrm{Pf}(F^{\overline{p}}).\end{aligned} \tag{B10}$$

$F^{\overline{p}}$ is defined as $F^{\overline{p}}_{1,1} = 0$, $F^{\overline{p}}_{1,r+1} = h_{m_p,m_r}$, and $F^{\overline{p}}_{r+1,s+1} = \tilde{f}_{rs} = f_{m_r,m_s} - f_{m_s,m_r}$ with $r, s \neq p$:

$$F^{\overline{p}} = \begin{pmatrix} 0 & h_{m_p,m_1} & h_{m_p,m_2} & h_{m_p,m_3} & \cdot\cdot(p)\cdot & h_{m_p,m_{2n}} \\ -h_{m_p,m_1} & 0 & \tilde{f}_{1,2} & \tilde{f}_{1,3} & \cdot\cdot(p)\cdot & \tilde{f}_{1,2n} \\ -h_{m_p,m_2} & \tilde{f}_{2,1} & 0 & \tilde{f}_{2,3} & \cdot\cdot(p)\cdot & \tilde{f}_{2,2n} \\ \cdot\cdot(p)\cdot & & & & \cdot\cdot(p)\cdot & \\ -h_{m_p,m_N} & \tilde{f}_{2n,1} & \tilde{f}_{2n,2} & \tilde{f}_{2n,3} & \cdot\cdot(p)\cdot & 0 \end{pmatrix}, \tag{B11}$$

where (p) denotes that the index p is skipped. The extension to more-broken-pairs states is also expected.

Equations (B6) and (B7) provide us with the overlap between the m-scheme basis state and the HFB wave function by computing the Pfaffian once. On the other hand, Bertsch and Robledo presented a simple formulation to obtain the overlap of the HFB wave functions of odd-mass nuclei for the projection method [35]. It is an extension to the overlap of the HFB wave functions of even-mass nuclei, and is obtained also by computing the Pfaffian once.

We presented Eqs. (B10) and (B11) for obtaining the overlap between m-scheme basis state and one-broken-pair wave function. Unfortunately, they require computing the $2n$ Pfaffians, which would make the computation time greater.

APPENDIX C: STOCHASTIC RECONFIGURATION

In the present VMC framework, many variables are optimized simultaneously to minimize the energy expectation values stochastically. Although the stochastic estimation of the gradient vector enables us to use the steepest gradient method, it is unstable due to the stochastic error. In order to stabilize the numerical calculation and to accelerate it, Sorrella introduced the stochastic reconfiguration (SR) method [7]. In this Appendix, we describe the details of the SR method with variation after the angular-momentum projection.

The angular-momentum projection obliges us to introduce complex numbers as variational parameters, while only real numbers are often used as variational parameters in the preceding works in condensed matter physics (e.g., [1]). Here, we describe the extension of the SR method of the projected wave function including complex numbers as variational parameters.

We define a derivative operator $\mathcal{O}_i$, which is diagonal in the m-scheme basis states, and its conjugate operator $\mathcal{O}_i^\dagger$ as

$$\begin{aligned}\mathcal{O}_i &= \sum_m |m\rangle \left[\frac{1}{\langle m|\psi_\alpha\rangle}\frac{\partial}{\partial\alpha_i}\langle m|\psi_\alpha\rangle\right]\langle m| \\ &= \sum_m |m\rangle O_i(m,\alpha)\langle m|, \\ \mathcal{O}_i^\dagger &= \sum_m |m\rangle \left[\frac{1}{\langle \psi_\alpha|m\rangle}\frac{\partial}{\partial\alpha_i^*}\langle \psi_\alpha|m\rangle\right]\langle m| \\ &= \sum_m |m\rangle O_i^*(m,\alpha)\langle m|, \end{aligned} \tag{C1}$$

with

$$\begin{aligned} O_i(m,\alpha) &= \frac{1}{\langle m|\psi_\alpha\rangle}\frac{\partial}{\partial\alpha_i}\langle m|\psi_\alpha\rangle, \\ O_i^*(m,\alpha) &= \frac{1}{\langle \psi_\alpha|m\rangle}\frac{\partial}{\partial\alpha_i^*}\langle \psi_\alpha|m\rangle, \end{aligned} \tag{C2}$$

and α denotes a set of variational parameters which are complex numbers. In the present work for the odd-mass case, the variational parameters are $\alpha = \{g_K, \alpha_{ij}, h_l, f_{kk'}\}$. These operators satisfy the following derivative equations:

$$\begin{aligned}\langle m|\mathcal{O}_i|\psi_\alpha\rangle &= \frac{\partial}{\partial\alpha_i}\langle m|\psi_\alpha\rangle \\ \langle\psi_\alpha|\hat{O}_i^\dagger|m\rangle &= \frac{\partial}{\partial\alpha_i^*}\langle\psi_\alpha|m\rangle = \langle m|\mathcal{O}_i|\psi_\alpha\rangle^*. \end{aligned} \tag{C3}$$

The normalized trial wave function is written as

$$|\overline{\psi}_\alpha\rangle = \frac{1}{\sqrt{\langle\psi_\alpha|\psi_\alpha\rangle}}|\psi_\alpha\rangle. \tag{C4}$$

The derivative of the normalized trial wave function with respect to α can be written as

$$\begin{aligned}\frac{\partial}{\partial\alpha_i}|\overline{\psi}_\alpha\rangle &= \left(\mathcal{O}_i - \frac{1}{2}\langle\mathcal{O}_i\rangle\right)|\overline{\psi}_\alpha\rangle, \\ \frac{\partial}{\partial\alpha_i^*}|\overline{\psi}_\alpha\rangle &= -\frac{1}{2}\langle\mathcal{O}_i^\dagger\rangle|\overline{\psi}_\alpha\rangle, \end{aligned} \tag{C5}$$

where we use the shorthand notation $\langle\mathcal{O}\rangle = \langle\overline{\psi}|\mathcal{O}|\overline{\psi}\rangle$.

The energy gradient g_i is obtained utilizing these derivative operators as

$$g_i \equiv \frac{\partial}{\partial\alpha_i^*}\langle\overline{\psi}|H|\overline{\psi}\rangle = \langle\mathcal{O}_i^\dagger H\rangle - \langle\mathcal{O}_i^\dagger\rangle\langle H\rangle, \tag{C6}$$

We evaluate $\langle\mathcal{O}_i^\dagger\rangle$, $\langle\mathcal{O}_i\rangle$, $\langle\mathcal{O}_i^\dagger\mathcal{O}_j\rangle$, and $\langle\mathcal{O}_i^\dagger H\rangle$ stochastically by

$$\begin{aligned}\langle\mathcal{O}_i^\dagger\rangle &= \frac{\langle\psi|\mathcal{O}_i^\dagger|\psi\rangle}{|\langle\psi|\psi\rangle|^2} = \frac{\sum_m\langle\psi|\mathcal{O}_i^\dagger|m\rangle\langle m|\psi\rangle}{\sum_m|\langle m|\psi\rangle|^2} \\ &= \frac{\sum_m|\langle\psi|m\rangle|^2 O_i^*(m,\alpha)}{\sum_m|\langle m|\psi\rangle|^2} \\ &= \sum_m p(m)O_i^*(m,\alpha), \end{aligned} \tag{C7}$$

where $p(m)$ is defined as $p(m) = |\langle m|\psi\rangle|^2/\sum_{m'}|\langle m'|\psi\rangle|^2$. The weighted summation $\sum_m p(m)$ is realized by the Markov chain Monte Carlo (MCMC) process in which $|m\rangle$ is generated obeying the probability $p(m)$. The energy is also evaluated in the same manner as

$$E_L(m) = \frac{\langle m|H|\psi\rangle}{\langle m|\psi\rangle}, \quad \langle H\rangle = \sum_m p(m)E_l(m). \tag{C8}$$

Other relevant values are evaluated as

$$\langle\mathcal{O}_i\rangle = \sum_m p(m)O_i(m,\alpha) = \langle\mathcal{O}_i^\dagger\rangle^*, \tag{C9}$$

$$\langle\mathcal{O}_i^\dagger\mathcal{O}_j\rangle = \sum_m p(m)O_i^*(m,\alpha)O_j(m,\alpha), \tag{C10}$$

$$\begin{aligned}\langle\mathcal{O}_i^\dagger H\rangle &= \frac{\sum_m\langle\psi|\mathcal{O}_i^\dagger|m\rangle\langle m|H|\psi\rangle}{\sum_m|\langle m|\psi\rangle|^2} \\ &= \sum_m p(m)O_i^*(m,\alpha)E_L(m), \end{aligned} \tag{C11}$$

$$\langle H\mathcal{O}_i\rangle = \sum_m p(m)E_L^*(m)O_i(m,\alpha). \tag{C12}$$

The derivative concerning the operator G is evaluated as

$$O_{\alpha_{ij}}(m,\alpha) = \frac{1}{\langle m|\psi\rangle}\frac{\partial}{\partial\alpha_{ij}}\langle m|e^{\sum_{i\leqslant j}\alpha_{ij}n_in_j}|\psi\rangle = \sum_{i\leqslant j} n_i^{(m)}n_j^{(m)} \tag{C13}$$

with $n_i^{(m)} = \langle m|n_i|m\rangle$.

The derivative concerning correlated pairs is

$$\begin{aligned} O_{f_{ij}}(m,\alpha) &= \frac{1}{\langle m|\psi\rangle}\frac{\partial}{\partial(f_m)_{ij}}\langle m|\psi\rangle \\ &= \frac{1}{\gamma_m 2^{N/2}(N/2)!\,\mathrm{Pf}(f_m)} \\ &\quad\times\left[-(f_m)_{ij}^{-1}\mathrm{Pf}(f_m)\gamma_m 2^{N/2}(N/2)!\right] \\ &= -(f_m)_{ij}^{-1} = -f_{m_im_j} \\ &= \frac{1}{2}\left[(f_m)_{ji}^{-1} - (f_m)_{ij}^{-1}\right]. \end{aligned} \tag{C14}$$

The derivative concerning the correlated-pair parameters of the J-projected energy is

$$\begin{aligned} O_{f_{kk'}}(m,\alpha) &= \frac{1}{\langle m|P_M^J|\phi\rangle}\frac{\partial}{\partial X_{ab}}\langle m|P_M^J|\phi\rangle \\ &= \frac{1}{\sum_{nK} g_K w_{nK}\langle m|R_n|\phi\rangle} \\ &\quad\times\sum_{nK} g_K w_{nK}\frac{\partial}{\partial X_{ab}}\langle m|R_n|\phi\rangle \\ &= \frac{1}{\sum_{nK} g_K w_{nK}\langle m|R_n|\phi\rangle}\sum_{nK} g_K w_{nK}\langle m|R_n|\phi\rangle \\ &\quad\times\left(-\sum_{i,j=1}^{N} R^T_{am_i}\{[(RXR^T)_m]^{-1}\}_{m_im_j}R_{m_jb}\right) \end{aligned} \tag{C15}$$

The derivative concerning the g_K is

$$\begin{aligned} O_{g_K}(m,\alpha) &= \frac{1}{\langle m|\psi\rangle}\frac{\partial}{\partial g_K}\langle m|\psi\rangle \\ &= \frac{1}{\sum_{nK'} g_{K'}w_{nK'}\langle m|R_n|\phi\rangle}\sum_n w_{nK}\langle m|R_n|\phi\rangle. \end{aligned} \tag{C16}$$

By combining these equations and the MCMC procedure, we can evaluate the energy gradient of the J-projected energy.

The norm of the small displacement of the $|\overline{\psi}\rangle$ caused by the small change of the variational parameters γ_i is

$$\begin{aligned} \Delta^2_{\mathrm{norm}} &= \||\overline{\psi}_{\alpha+\gamma}\rangle - |\overline{\psi}_\alpha\rangle\|^2 \\ &= \sum_{ij}\gamma_i^*\gamma_j\frac{\partial}{\partial\alpha_i^*}\frac{\partial}{\partial\alpha_j}\langle\overline{\psi}|\overline{\psi}\rangle \\ &= \sum_{ij}\gamma_i^* S_{ij}\gamma_j \end{aligned} \tag{C17}$$

with the overlap matrix S_{ij},

$$S_{ij} = \langle\mathcal{O}_i^\dagger\mathcal{O}_j\rangle - \langle\mathcal{O}_i^\dagger\rangle\langle\mathcal{O}_j\rangle, \tag{C18}$$

which is Hermitian and positive semidefinite [36].

In the steepest-gradient method, the small displacement is taken as the derivative of energy as

$$\gamma_i = -\Delta t\frac{\partial\langle H\rangle}{\partial\alpha_i^*} = -\Delta t g_i. \tag{C19}$$

On the other hand, in the SR method, the small displacement is taken as the product of the inverse of S_{ij} and derivative of energy as

$$g_i' = -\Delta t\sum_j S_{ij}^{-1}g_j. \tag{C20}$$

By using the inverse of S_{ij} the direction with the small norm of S_{ij}, or the direction causing small displacement, is taken as large step width and vice versa. In this work, we typically take $\Delta t = 0.2$.

In order to stabilize the SR method further, we apply two modifications to the overlap matrix S_{ij} following Ref. [1]. One is the scaling of its diagonal matrix elements. We replace the overlap matrix by the scaled one,

$$S'_{ij} = (1+\epsilon\delta_{ij})S_{ij}, \tag{C21}$$

where ϵ is a small constant. This modification makes the overlap matrix positive definite and stable even if S_{ij} is calculated stochastically including a certain error [37]. In this work, we typically take $\epsilon = 0.01/\sqrt{i}$, where i is the number of iterations.

The other method to stabilize the SR method is the truncation of the redundant directions by introducing the cutoff of the small eigenvalues of the overlap matrix. As it is Hermitian, we can diagonalize the overlap matrix by

$$S_{ij} = \sum_k U_{ik}\lambda_k U_{kj}^\dagger. \tag{C22}$$

The redundancy of the variational-parameter space causes zero or small eigenvalues of the overlap matrix. Besides, small eigenvalues with statistical errors cause instability in evaluating the inverse matrix in Eq. (C20). In order to avoid the problem, we replace $1/\lambda_i$ by 0 for $\lambda_i < \epsilon_{\mathrm{cut}}$. In this work, we typically take $\epsilon_{\mathrm{cut}} = 2/\sqrt{i}\times 10^{-4}$, where i is the number of iterations. Thus,

$$\gamma_k = -\Delta t\sum_l S_{kl}^{-1}g_l = -\Delta t\sum_{il}\frac{1}{\lambda_i}U_{ki}U_{il}^\dagger g_l \tag{C23}$$

is replaced by

$$\gamma_k = -\Delta t\sum_{il}\Theta(\lambda_i-\epsilon_{\mathrm{cut}})\frac{1}{\lambda_i}U_{ki}U_{il}^\dagger g_l, \tag{C24}$$

where $\Theta(x)$ is the Heaviside function.

As a summary, we iteratively shift the variational parameters by adding the direction provided by Eq. (C20) in the SR method. It is expected to decrease the energy expectation value and, at the same time, to suppress the norm of the displacement of the wave functions by removing the effect of the redundancy of the variational parameters. This procedure is iterated until the energy converges.

[1] D. Tahara and M. Imada, J. Phys. Soc. Jpn. **77**, 114701 (2008).
[2] F. Ferrari, A. Parola, S. Sorella, and F. Becca, Phys. Rev. B **97**, 235103 (2018).
[3] T. Misawa, K. Nakamura, and M. Imada, Phys. Rev. Lett. **108**, 177007 (2012).
[4] V. R. Pandharipande, S. C. Pieper, and R. B. Wiringa, Phys. Rev. B **34**, 4571 (1986).
[5] J. Carlson, S. Gandolfi, F. Pederiva, S. C. Pieper, R. Schiavilla, K. E. Schmidt, and R. B. Wiringa, Rev. Mod. Phys. **87**, 1067 (2015).
[6] T. Mizusaki and N. Shimizu, Phys. Rev. C **85**, 021301(R) (2012).
[7] S. Sorella, Phys. Rev. B **64**, 024512 (2001).
[8] M. Bajdich, L. Mitas, G. Drobny, L. K. Wagner, and K. E. Schmidt, Phys. Rev. Lett. **96**, 130201 (2006).
[9] E. Caurier, G. Martnez-Pinedo, F. Nowacki, A. Poves, and A. P. Zuker, Rev. Mod. Phys. **77**, 427 (2005).
[10] A. Petrovici, Nucl. Phys. A **704**, 144c (2002).
[11] B. Bally, B. Avez, M. Bender, and P.-H. Heenen, Phys. Rev. Lett. **113**, 162501 (2014).
[12] P. Ring and P. Schuck, *The Nuclear Many-Body Problem*, (Springer-Verlag, New York, 1980).
[13] T. Mizusaki and M. Imada, Phys. Rev. B **69**, 125110 (2004).
[14] G. E. Scuseria, C. A. Jimenez-Hoyos, T. M. Henderson, K. Samanta, and J. K. Ellis, J. Chem. Phys. **135**, 124108 (2011).
[15] C. Yannouleas and U. Landman, J. Phys.: Condens. Matter **14**, L591 (2002).
[16] H. J. Mang, Phys. Rep. **18**, 325 (1975).
[17] A. L. Goodman, Phys. Rev. C **60**, 014311 (1999).
[18] E. Ha, M.-K. Cheoun, H. Sagawa, and W. Y. So, Phys. Rev. C **97**, 064322 (2018).
[19] C. W. Johnson, W. E. Ormand, and P. G. Krastev, Comput. Phys. Commun. **184**, 2761 (2013).
[20] N. Shimizu, T. Mizusaki, and K. Kaneko, Phys. Lett. B **723**, 251 (2013).
[21] M. Lingle and A. Volya, Phys. Rev. C **91**, 064304 (2015).
[22] W. H. Press, S. A. Teukolsky, W. T. Vetterling, and B. P. Flannery, *Numerical Recipes in FORTRAN* (Cambridge University Press, Cambridge, 1992).
[23] T. Otsuka, M. Honma, T. Mizusaki, N. Shimizu, and Y. Utsuno, Prog. Part. Nucl. Phys. **47**, 319 (2001).
[24] M. Honma, T. Otsuka, B. A. Brown, and T. Mizusaki, Eur. Phys. J. A **25**, 499 (2005).
[25] N. Shimizu, arXiv:1310.5431.
[26] E. Caurier, J. L. Egido, G. Martinez-Pinedo, A. Poves, J. Retamosa, L. M. Robledo, and A. P. Zuker, Phys. Rev. Lett. **75**, 2466 (1995).
[27] A. Poves and G. M. Pinedo, Phys. Lett. B **430**, 203 (1998).
[28] N. Shimizu, T. Abe, Y. Tsunoda, Y. Utsuno, T. Yoshida, T. Mizusaki, M. Honma, and T. Otsuka, Prog. Theor. Exp. Phys. **2012**, 01A205 (2012); N. Shimizu, T. Abe, M. Honma, T. Otsuka, T. Togashi, Y. Tsunoda, Y. Utsuno, and T. Yoshida, Phys. Scr. **92**, 063001 (2017).
[29] G. Puddu, Euro. Phys. J. A **31**, 163 (2007).
[30] K. Hagino, P.-G. Reinhard, and G. F. Bertsch, Phys. Rev. C **65**, 064320 (2002).
[31] T. Mizusaki, Phys. Rev. C **70**, 044316 (2004).
[32] M. Imada and T. Kashima, J. Phys. Soc. Jpn. **69**, 2723 (2000).
[33] N. Shimizu, Y. Utsuno, T. Mizusaki, T. Otsuka, T. Abe, and M. Honma, Phys. Rev. C **82**, 061305(R) (2010).
[34] T. Mizusaki and M. Imada, Phys. Rev. C **65**, 064319 (2002); **67**, 041301(R) (2003).
[35] G. F. Bertsch and L. M. Robledo, Phys. Rev. Lett. **108**, 042505 (2012).
[36] I. Glasser, N. Pancotti, M. August, I. D. Rodriguez, and J. I. Cirac, Phys. Rev. X **8**, 011006 (2018).
[37] S. Sorella, M. Casula, and D. Rocca, J. Chem. Phys. **127**, 014105 (2007).